Importance of Loops of Mitochondrial ADP/ATP Carrier for Its Transport Activity Deduced from Reactivities of Its Cysteine Residues with the Sulfhydryl Reagent Eosin-5-maleimide

Eiji Majima,[†,§] Yasuo Shinohara,[‡] Nana Yamaguchi,[‡] Yeong-Man Hong,[§] and Hiroshi Terada*[,‡]

Faculty of Pharmaceutical Sciences, University of Tokushima, Shomachi-1, Tokushima 770, Japan, and APRO Life Science Institute, Kurosaki, Naruto 772, Japan

Received March 17, 1994; Revised Manuscript Received June 6, 1994[⊕]

ABSTRACT: The effects of various compounds such as the transport substrate ADP and the transport inhibitors carboxyatractyloside (CATR) and bongkrekic acid (BKA) on the labeling of cysteine residues in the ADP/ATP carrier of bovine heart submitochondrial particles by the SH reagent eosin-5-maleimide (EMA) were studied. Of the four cysteine residues in the carrier, the labeling of Cys^{159} by EMA progressed predominantly and rapidly, and those of Cys^{56} and Cys^{256} moderately, but Cys^{128} was not labeled, as we reported previously [Majima, E., et al. (1993) *J. Biol. Chem. 268*, 22181–22187]. ADP inhibited the labelings of Cys^{56}, Cys^{159}, and Cys^{256} by EMA. BKA markedly inhibited the labeling of Cys^{159} by EMA, and also the labeling of Cys^{256}, but did not affect the labeling of Cys^{56}, suggesting that it binds from the matrix side to a region close to Cys^{159} in the second loop facing the matrix space. CATR completely inhibited the labeling by EMA when added on the cytosolic side, but had no effect when added on the matrix side. From these results, the conformational changes of the carrier induced by CATR, BKA, and ADP are discussed. Furthermore, a mechanism of adenine nucleotide transport through the ADP/ATP carrier in association with change in its conformation is proposed.

The ADP/ATP carrier in the inner mitochondrial membrane mediates the exchange transports of ADP and ATP. Despite extensive studies on its structure in the membrane and its transport function (Klingenberg, 1993; Brandolin et al., 1993), the transport mechanism of these nucleotides in terms of its structure is not fully understood. In a previous study, we examined the labeling by the maleimide-type SH reagents EMA[1] and NEM of the four cysteine residues Cys^{56}, Cys^{128}, Cys^{159}, and Cys^{256} of the ADP/ATP carrier in bovine heart submitochondrial particles (Majima et al., 1993). EMA is a bulky divalent anion and so is membrane-impermeable, interacting with the carrier only from the matrix side in submitochondrial particles, whereas NEM is electrically neutral and membrane permeable, interacting with the carrier from the matrix side both in mitochondria and in submitochondrial particles. These SH reagents clearly distinguish the environments of the four cysteine residues in the carrier and differ in their reactivities with these cysteine residues. From labeling studies with EMA and NEM, we deduced the locations of these cysteine residues in the membrane and suggested that the three loops of the carrier containing Cys^{56}, Cys^{159}, and Cys^{256}, respectively, are located on the matrix side and that the loop containing Cys^{159} is the most important for the adenine nucleotide transport activity (Majima et al., 1993). Our results are consistent with the six-transmembrane model (three-repeat domain structure) of the ADP/ATP carrier (Klingenberg, 1989; Saraste & Walker, 1982).

As an extension of this study, we examined the effects of ADP, BKA, and CATR on the labeling by EMA of the cysteine residues in the ADP/ATP carrier to determine the relationship between its conformational states and its reactivity of EMA. We refer to the three loops facing the matrix space as loops M1, M2, and M3 in order of their amino acid sequences: loop M1 consists of the sequence Glu^{29}–Arg^{71} containing Cys^{56}, loop M2 that of Asp^{134}–Gln^{174} containing Cys^{159}, and loop M3 that of Asp^{231}–Lys^{271} containing Cys^{256}. We suggest in this paper that loop M2 is the primary binding site of the transport substrates and transport inhibitors and that the states of these three loops govern the conformations of the carrier, regulating the transport activity. We also propose a model of ADP transport mediated by the dimeric ADP/ATP carrier based on the six-transmembrane model of its structure.

MATERIALS AND METHODS

Reagents. EMA was purchased from Molecular Probes (Eugene, OR), and BKA was a gift from Prof. Duine, Delft University of Technology. CATR was obtained from Sigma (St. Louis). Lysyl endopeptidase and nucleotides were from Wako Pure Chemical Industries (Osaka), and hydroxylapatite was from Bio-Rad Laboratories (Richmond). Reagents for HPLC were from Kanto Chemical Co. (Tokyo).

Preparation of Bovine Heart Submitochondrial Particles. Submitochondrial particles were prepared from bovine heart mitochondria (Smith, 1967) according to Hansen and Smith (1964) as described before (Majima et al., 1993). CATR-preloaded submitochondrial particles were prepared by the same method from mitochondria that had been incubated with 4 nmol of CATR/mg of protein at 25 °C for 10 min.

Labeling of ADP/ATP Carrier by EMA. For examination of the effects of various compounds such as ADP, CATR, and BKA on the labeling of the ADP/ATP carrier by EMA,

* To whom correspondence should be addressed.
† University of Tokushima.
§ APRO Life Science Institute.
⊕ Abstract published in *Advance ACS Abstracts,* July 15, 1994.
[1] Abbreviations: EMA, eosin-5-maleimide; NEM, *N*-ethylmaleimide; EDTA, ethylenediaminetetraacetic acid; SDS–PAGE, sodium dodecyl sulfate–polyacrylamide gel electrophoresis; Tris, tris(hydroxymethyl)-aminomethane; ATR, atractyloside; CATR, carboxyatractyloside; BKA, bongkrekic acid; Pal-CoA, palmitoyl-CoA; HPLC, high-performance liquid chromatography; DTT, dithiothreitol; RCAM, ADP/ATP carrier reduced and carboxamidomethylated; REMA, ADP/ATP carrier reduced and modified with EMA.

0006-2960/94/0433-9530$04.50/0

submitochondrial particles suspended in medium consisting of 250 mM sucrose, 1 μg of oligomycin/mg of protein, 0.2 mM EDTA, and 10 mM Tris-HCl buffer, pH 7.2, were first preincubated with these compounds for 10 min and then incubated with EMA for various periods in a total volume of 100 μL at 0 °C in the dark. Labeling with EMA was terminated by addition of 1 M DTT to a final concentration of 50 mM. The particles were then subjected to SDS–PAGE in 15% polyacrylamide gel by the method of Laemmli (1970). The fluorescence intensity of the ADP/ATP carrier labeled with EMA in the gel was measured with excitation at 530 nm in a Shimadzu chromatoscanner, CS-9000.

Determination of Cysteine Residues Labeled with EMA. Cysteine residues of the ADP/ATP carrier labeled with EMA were determined as described previously (Majima et al., 1993). The carrier was isolated from submitochondrial particles treated with 100 μM EMA for 10 min at 0 °C in the dark. The protein fraction obtained by hydroxylapatite chromatography was precipitated with acetone, denatured with guanidine hydrochloride, reduced with DTT, and carboxamidomethylated with iodoacetamide. By these treatments, all the cysteine residues that had not reacted with EMA were alkylated. After isolation by chromatography on a column of G3000SW$_{XL}$ (0.78 × 30 cm, Tosoh Co., Tokyo), the labeled ADP/ATP carrier was digested with lysyl endopeptidase (2% w/w) at 37 °C for 24 h, and the peptides derived from the carrier were separated by reversed-phase HPLC on a TSK gel ODS-120T column (0.46 × 15 cm, Tosoh) with a linear gradient of 12–52% acetonitrile containing 0.05% trifluoroacetic acid at a flow rate of 1.0 mL/min in 80 min. The elution profile was monitored as the absorbance at 210 nm, and subsequently as fluorescence at 555 nm with excitation at 520 nm.

The amounts of cysteine residues labeled by EMA were determined from the decreases in heights of the chromatographic elution peaks due to the carboxamidomethylated peptide fragments that had not been labeled by EMA. For identification of these peptide fragments in the chromatographic elution profile, the isolated ADP/ATP carrier was denatured with guanidine hydrochloride and reduced with DTT, and then all the cysteine residues were modified with iodoacetamide and EMA. These modified carriers, referred to as RCAM and REMA, respectively, were digested with lysyl endopeptidase, and the resulting peptide fragments were subjected to reversed-phase HPLC as described above. The amino acid sequences of the labeled peptide fragments were then analyzed. Details of these procedures were described in our previous paper (Majima et al., 1993).

Protein Determination. The protein concentrations of mitochondria and submitochondrial particles were determined with a BCA protein assay kit (Pierce, Rockford) in the presence of 1% SDS using bovine serum albumin as a standard.

RESULTS

Time Course of Labeling by EMA of the ADP/ATP Carrier in the Presence of Various Compounds. As shown in Figure 1, incubation of the bovine heart submitochondrial particles with EMA resulted in the specific labeling of a 30-kDa protein detected by SDS–PAGE. This protein was the ADP/ATP carrier, as determined by amino acid sequencing (Majima et al., 1993). We found that various compounds such as transport substrates and transport inhibitors suppressed the labeling of the carrier by EMA. The effects of ADP on its labeling at 0 and 25 °C are shown in Figure 1. As shown in Figure 2, at 0 °C in the absence of test compounds, the labeling by

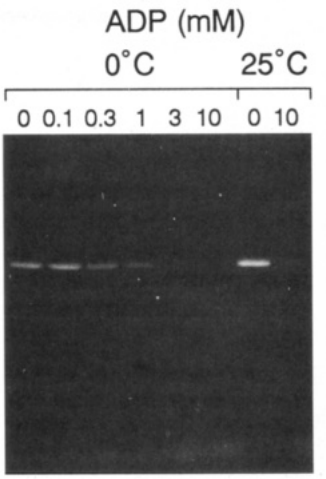

FIGURE 1: Effect of ADP on labeling of the ADP/ATP carrier in bovine heart submitochondrial particles by EMA. Submitochondrial particles prepared from bovine heart mitochondria were suspended at 10 mg of protein/mL in medium consisting of 250 mM sucrose, 1 μg of oligomycin/mg of protein, 0.2 mM EDTA, and 10 mM Tris-HCl buffer (pH 7.2) in a total volume of 100 μL. They were first incubated with ADP for 10 min at 0 or 25 °C and then treated with 100 μM EMA for 30 s at 0 °C or for 10 s at 25 °C. After termination of the labeling by addition of DTT (final concentration 50 mM), samples of 25 μg of protein of particles were subjected to SDS–PAGE and fluorography.

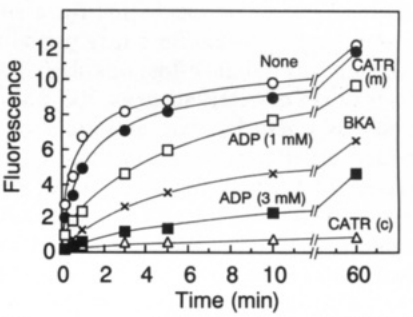

FIGURE 2: Time courses of labeling of the ADP/ATP carrier in submitochondrial particles by EMA in the presence of various compounds. Before incubation with EMA, submitochondrial particles (10 mg of protein/mL) were incubated for 10 min at 0 °C with 100 μM CATR, 100 μM BKA, or 1 or 3 mM ADP. The effects of CATR added to the matrix side [CATR(m)] and in CATR-preloaded submitochondrial particles [CATR(c)] were examined. After termination of labeling by EMA, the particles were subjected to SDS–PAGE, and relative labelings were determined by measurement of the fluorescent intensity of the band labeled by EMA.

EMA proceeded very rapidly within the first 2 min, and then slower, and after 10 min the labeling was 82% of the maximum attained after 60 min. Amino acid sequence analyses of the peptide fragments containing labeled cysteine residues showed that the first rapid labeling was due to specific labeling of Cys^{159}, and the second slower labeling to the labelings of Cys^{56} and Cys^{256}, as we reported previously (Majima et al., 1993). No labeling of Cys^{128} was observed. The labeling proceeded slower than that reported previously, because in the present study the EMA concentration was 100 μM, which was lower than that used previously (400 μM) to allow more sensitive detection of the effects of test compounds on the labeling by EMA. We examined the effects of various compounds on the EMA labeling by preincubation of the particles (10 mg of protein/mL) with these compounds for 10 min at 0 °C, and then incubation with EMA for various periods.

As shown in Figure 2, 100 μM BKA and 3 mM ADP greatly suppressed the labeling of cysteine residues in the ADP/ATP carrier at all periods of incubation, but the labeling gradually

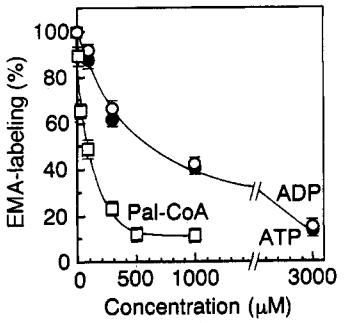

FIGURE 3: Effects of ADP, ATP, and Pal-CoA on the labeling of the ADP/ATP carrier by EMA. Experimental conditions were as for Figure 1. Submitochondrial particles at 10 mg of protein/mL were incubated with 100 μM EMA for 30 s at 0 °C after incubation for 10 min with various concentrations of ADP (open circles), ATP (closed circles), and Pal-CoA (open squares). The values (with error bars) are means for three or more separate runs.

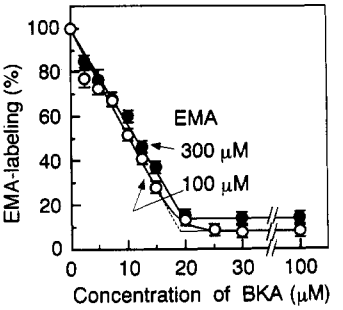

FIGURE 4: Inhibitory effect of BKA on the labeling of the ADP/ATP carrier by EMA at 0 °C. Experimental conditions were as for Figures 1 and 3. The concentrations of EMA used for labeling were 100 and 300 μM. The values (with error bars) are means for two separate runs.

increased with increase in the incubation period. As the labeling without these compounds proceeded first rapidly, and then gradually, their inhibitory effects were more significant in a short period of incubation than in a longer one. For instance, the labelings with 100 μM BKA and 3 mM ADP were both about 10% of that in their absence after 30 s, but about 45% and 25%, respectively, of the latter after 10 min. The inhibitory effect of a lower concentration of 1 mM ADP was also more significant on incubation for a short period such as 30 s than on incubation for a long period such as 10 min. Even though only a slight effect was observed with even lower concentrations of ADP such as 300 μM with long incubation periods, these low concentrations of ADP still showed considerable effects in short incubation periods such as 30 s, as described later (cf. Figure 3). CATR at 100 μM had no appreciable effect on the labeling when added on the matrix side, but a very strong inhibitory effect when added on the cytosolic side. The latter result is consistent with a previous report (Houstek & Pedersen, 1985).

Effects of Various Compounds on EMA Labeling of Cys^{159}. We next examined the effects of various compounds on the labeling of Cys^{159} by EMA, with which it predominantly interacts (Majima et al., 1993). For this, we preincubated the particles (10 mg of protein/mL) for 10 min with test compounds at various concentrations, and then incubated them with 100 μM EMA for 30 s at 0 °C. The effects of test compounds on the labeling were determined by the fluorescent intensity of the labeled EMA on SDS–PAGE. We confirmed by the elution profiles on reversed-phase HPLC and amino acid sequencing of the peptide fragments labeled by EMA that this period of incubation really caused specific labeling of Cys^{159} and that the test compounds inhibited the labeling of Cys^{159}. ATP and Pal-CoA, as well as ADP and BKA, inhibited the labeling of Cys^{159}. As shown in Figure 3, the inhibitory effects of ATP and ADP were very similar and were related hyperbolically with their concentrations. In contrast, as shown in Figure 4, the inhibitory effect of BKA was almost linearly related with its concentration up to a certain concentration, above which the inhibition became constant, owing to its much stronger binding than ADP and ATP to the carrier. BKA at 20 μM (2 nmol/mg of protein) or more inhibited the labeling by EMA about 90%, and its minimal concentration for this 90% inhibition was determined as 1.9 nmol of BKA/mg of protein, which is about the same as that required for its inhibition of ADP transport in submitochondrial particles (Lauquin et al., 1977).

We determined the concentrations and amounts of the test compounds necessary for 50% inhibition of the labeling by 100 μM EMA (IC_{50} and IA_{50} values, respectively), and results are summarized in Table 1. Of the compounds tested, BKA and Pal-CoA showed the most potent inhibitory effects, their IA_{50} values (1.0 and 6.7 nmol/mg of protein, respectively) being consistent with those for 50% inhibition of ADP transport in submitochondrial particles determined from the results reported by Lauquin et al. (1977). The effect of CATR on the matrix side was too low to allow determination of its inhibitory potency. The order of the inhibitory effects, BKA > Pal-CoA ≫ ATP = ADP, is well consistent with the binding affinities of these compounds to the carrier (Lauquin et al., 1977; Klingenberg, 1980). Therefore, their inhibitory potencies can be regarded as dependent on their specific binding abilities.

Table 1: Inhibitory Effects of Various Compounds on the Labeling by EMA of the ADP/ATP Carrier in Submitochondrial Particles[a]

addition	IC_{50}[b] (μM)	IA_{50}[c] (nmol/mg of protein)
ATP	640	64
ADP	660	66
CATR	ND[d]	ND[d]
BKA	10	1.0
Pal-CoA	67	6.7

[a] Submitochondrial particles were suspended at 10 mg of protein/mL in medium consisting of 250 mM sucrose, 1 μg of oligomycin/mg of protein, 0.2 mM EDTA, and 10 mM Tris-HCl buffer (pH 7.2). The suspensions were preincubated with test compounds at five different concentrations at 0 °C for 10 min and then treated with 100 μM EMA for 30 s at 0 °C, followed by addition of DTT (final concentration 50 mM). The particles were subjected to SDS–PAGE, and the labeling of the ADP/ATP carrier by EMA was determined by measurement of the fluorescence intensity of the band in the gel with excitation at 530 nm. [b] Concentration requiring for 50% inhibition of the labeling by EMA. [c] Amount requiring for 50% inhibition of the labeling. [d] Not determined due to very weak activity.

These compounds also inhibited labeling by EMA at concentrations other than 100 μM. As shown in Figure 4, the inhibitory effect of BKA on the labeling by 300 μM EMA was almost the same as that with 100 μM EMA with a similar titration point of 2.0 nmol/mg of protein. However, the residual labeling level (about 15%) was higher than that with 100 μM EMA (10%) due to further progress of the labelings of cysteine residues other than Cys^{159} by the higher concentration of EMA. Figure 5 shows the effect of ADP on the labelings by various concentrations of EMA in 30 s. As the effect of ADP was much lower than that of BKA, we set the amount of submitochondrial particles at 2 mg of protein/mL, which was less than that (10 mg of protein/mL) for Figure 3. This condition affords more sensitive detection of the weak effect of ADP at lower concentrations of ADP and EMA than those used in Figure 3, due to their higher amounts relative to the amount of carrier. The inhibitory effect of ADP, which

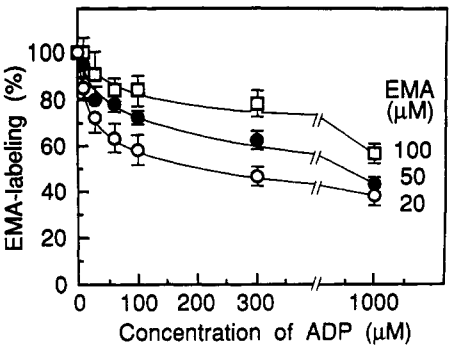

FIGURE 5: Effect of ADP on labeling of the ADP/ATP carrier by various concentrations of EMA. Submitochondrial particles (2 mg of protein/mL) were preincubated with various concentrations of ADP for 10 min and then incubated with various concentrations of EMA for 30 s at 0 °C. The values (with error bars) are means for three or more separate runs.

was hyperbolically related with its concentration, increased with decrease in the EMA concentration, indicating that its binding competes with that of EMA. The binding of ATP also competed with that of EMA (data not shown).

Cysteine Residues Protected by BKA and ADP from EMA Labeling after a Long Incubation Time. As described above, incubation of the submitochondrial particles with 100 μM EMA for 30 s at 0 °C resulted in the specific labeling of Cys^{159} of the ADP/ATP carrier. It was of interest to determine the effects of various compounds on the labelings by EMA of cysteine residues other than Cys^{159} of the carrier. Therefore, we examined the effects of preincubations with the transport substrate ADP and transport inhibitor BKA for 10 min at 0 °C on labeling of submitochondrial particles (10 mg of protein/mL) with EMA for the sufficiently long period of 10 min to label Cys^{56} and Cys^{256} as well as Cys^{159}. After the incubation, we isolated the carrier from the submitochondrial particles, reduced it with DTT, and carboxamidomethylated it with iodoacetamide. We then prepared peptide fragments from the labeled ADP/ATP carrier by digestion with lysyl endopeptidase and monitored their elution profiles on reversed-phase HPLC to determine the amounts of labeling by EMA.

We examined the effects of various concentrations of BKA and ADP on the labelings of the four cysteine residues of the ADP/ATP carrier. The effect of BKA was constant above its titration point (about 20 μM, cf. Figure 4). Although the effects of various concentrations of ADP were essentially the same, as expected from the results in Figure 5, its effect was greater at higher concentrations such as 3 mM, which was 5 times its IC_{50}, due to its weaker affinity than BKA to the carrier. Thus analyses of the effect of ADP at low concentrations were difficult. However, we could determine the effects of ADP at low concentrations such as 50 μM using submitochondrial particles at 2 mg of protein/mL, which was 1/5 of the concentration used in standard conditions (cf. Figure 5), and we confirmed that its effects on Cys^{56}, Cys^{159}, and Cys^{256} were qualitatively the same as those at higher concentrations such as 3 mM. Typical results on the effects of 100 μM BKA and 3 mM ADP determined by reversed-phase HPLC are described below.

Figure 6A shows the elution profile of the peptide fragments derived from the ADP/ATP carrier that had been alkylated with iodoacetamide. By this treatment, all the cysteine residues in the carrier were carboxamidomethylated. We refer to the reduced and carboxamidomethylated carrier as RCAM. In this elution profile, monitored as absorbance at 210 nm, the peaks of peptide fragments Gly^{147}–Lys^{162}, Gly^{245}–Lys^{259}, Gln^{49}–Lys^{62}, and Gln^{107}–Lys^{146} contained Cys^{159}, Cys^{256},

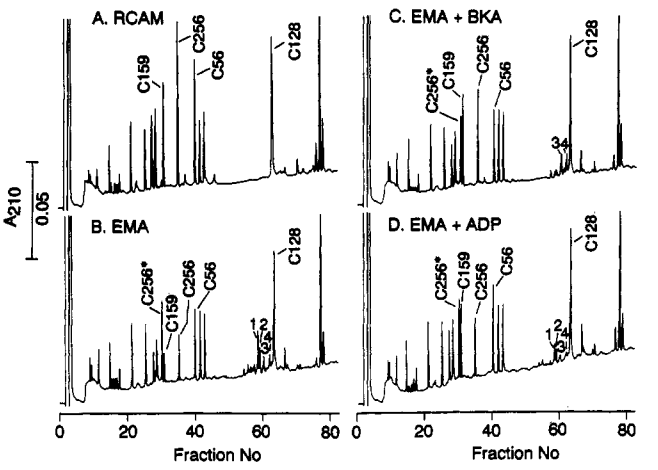

FIGURE 6: HPLC profiles of the peptide fragments derived from EMA-labeled ADP/ATP carrier in the presence or absence of BKA or ADP. The isolated carrier was denatured with 6 M guanidine hydrochloride, reduced with DTT, and then modified with iodoacetamide (A, RCAM). Submitochondrial particles (10 mg of protein/mL) were treated with EMA for 10 min without (B) or with preincubation for 10 min with 100 μM BKA (C) or 3 mM ADP (D) at 0 °C. C56, C128, C159, and C256 are peaks of peptide fragments containing Cys^{56}, Cys^{128}, Cys^{159}, and Cys^{256}, respectively, not labeled with EMA. The peak with an asterisk (C256*) had the same sequence as that of C256 (Majima et al., 1993). Peaks 1–4 are major fluorescent peaks due to peptide fragments labeled with EMA (cf. Figure 8).

Cys^{56}, and Cys^{128}, respectively, as we reported previously (Majima et al., 1993). These four peptides of RCAM not labeled by EMA are referred to as C159, C256, C56, and C128, respectively. In the elution profile of the isolated ADP/ATP carrier which had been reduced and completely labeled with EMA, referred to as REMA, these peaks were not seen, but instead, new peaks due to peptide fragments containing cysteine residues labeled with EMA were observed, as described below (cf. Figure 8). These peptides labeled by EMA are referred to as E56, E128, E159, and E256.

When the membrane-bound carrier was labeled by EMA, the height of the peak due to C159 was decreased greatly, and those of the peaks of C56 and C256 plus C256* [the peptide fragment containing the same amino acid sequence as that of C256, but appearing only when the membrane-bound carrier was treated with EMA, cf. Majima et al. (1993)] decreased slightly, but that of the C128 peak did not change (Figure 6B). Figure 6C shows the elution profile of the peptide fragments from the membrane-bound carrier treated with EMA after preincubation with BKA. The peak heights of C159 and C256 plus C256* were not significantly different from those of RCAM, but were different from those without BKA treatment, indicating that Cys^{159} and Cys^{256} of the BKA-bound carrier were scarcely labeled with EMA. In contrast, the peak height of C56 was similar to that of the membrane-bound carrier treated with EMA alone (cf. Figure 6B). When the membrane-bound carrier was preincubated with ADP, the peak heights due to C56, C159, and C256 plus C256* were lower than those from RCAM, as shown in Figure 6D, but these peaks were still higher than those after treatment with EMA alone (cf. Figure 6B). As EMA is fluorophoric, the peptide fragments bound by EMA gave fluorescent peaks. The major peaks of fluorescence are numbered peaks 1–4 in order of their elutions (Figure 6B–D).

As the peptides labeled by EMA showed complicated elution profiles (cf. Figure 8), we determined the relative amounts of cysteine residues labeled with EMA from the decreases in heights of the peaks due to the unlabeled peptides C56, C128, C159, and C256 plus C256*. There was no detectable labeling

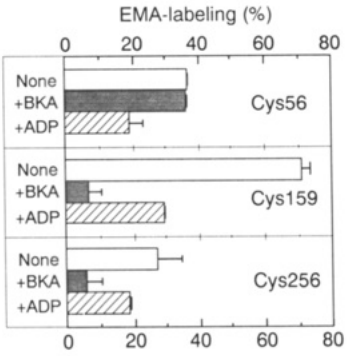

FIGURE 7: Effects of BKA and ADP on labeling by EMA of cysteine residues in the membrane-bound ADP/ATP carrier. Submitochondrial particles (10 mg/mL) were preincubated with 100 μM BKA or 3 mM ADP for 10 min and then incubated with EMA (100 μM) for 10 min at 0 °C. Amounts of labeling by EMA were determined from the decreases in the peak heights of the peptides containing cysteine residues not labeled with EMA shown in Figure 6, taking those of RCAM as references. Values are means ± SD for three separate experiments.

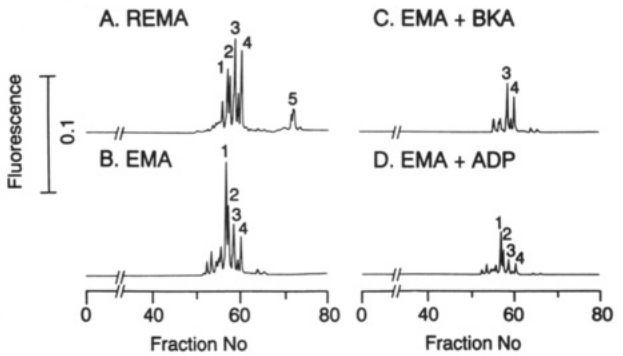

FIGURE 8: HPLC profiles of fluorescent peptide fragments derived from membrane-bound carrier treated with EMA in the presence or absence of BKA or ADP. Reversed-phase HPLC was performed with peptides derived from the isolated carrier labeled with EMA (A, REMA) and from the carrier in submitochondrial particles treated with EMA for 10 min in the absence (B, EMA) or presence of 100 μM BKA (C, EMA + BKA) or 3 mM ADP (D, EMA + ADP). These elution profiles were monitored as fluorescence at 555 nm with excitation at 520 nm after monitoring the absorbance at 210 nm (cf. Figure 6). Major fluorescent peaks are numbered peaks 1–5 in order of their elution.

of Cys^{128} by EMA with or without ADP or BKA. As shown in Figure 7, the relative amounts of Cys^{56}, Cys^{159}, and Cys^{256} labeled by EMA in the absence of BKA or ADP were 37%, 72%, and 27%, respectively, of those of RCAM. After preincubation with BKA, these values changed to 36%, 6%, and 6%, and after preincubation with ADP to 19%, 29%, and 18%, respectively. These results showed that BKA strongly inhibited the EMA labeling of Cys^{159} and Cys^{256}, but not that of Cys^{56}, whereas ADP inhibited the labelings of all these cysteine residues.

Figure 8 shows the fluorescent elution profiles of peptides derived from the carrier labeled by EMA for 10 min, monitored simultaneously with the absorbance at 210 nm shown in Figure 6. In the elution profile of the peptide fragments derived from REMA (Figure 8A), peaks 1 and 2 were determined to be due to E159, and peaks 3 and 4 to E56, while peak 5 was due to E128 (Majima et al., 1993). The plural peaks of single peptides modified by EMA in the chromatogram were due to the unstable chemical nature of the maleimide ring (Smyth, 1964) of the EMA bound to these peptides, and part of the elution profile of E256 is hidden by its overlapping with peaks 1–4 (Majima et al., 1993). Figure 8B shows the elution profile of the peptide fragments derived from the membrane-bound ADP/ATP carrier treated with EMA. The elution profile was similar to that of REMA, but peak 5 was not detectable due to lack of reactivity of Cys^{128} in the membrane-bound carrier with EMA (Majima et al., 1993). Preincubation of the membrane-bound carrier with BKA almost completely inhibited the appearance of peaks 1 and 2, but not peaks 3 and 4 (Figure 8C), and preincubation with ADP caused smaller fluorescent heights of peaks 1–4 than those with the membrane-bound carrier treated with EMA alone (Figure 8D). Although we could not determine the amount of labeling quantitatively from the increase in the fluorescent peak heights due to labeled peptide fragments, these results were qualitatively in line with those determined from decreases in the peak heights due to unlabeled peptide fragments (Figure 7).

DISCUSSION

Chemical modification of cysteine residues provides useful information about structural features of proteins in relation to their activity. We found that the divalent anionic SH reagent EMA specifically labels the cysteine residues in the ADP/ATP carrier of bovine submitochondrial particles from the matrix side, in association with its inhibition of ADP transport (Majima et al., 1993), although no particular cysteine residue(s) of the carrier has been suggested to be essential for its transport activity (Majima et al., 1993; Nelson et al., 1993). We found that, of the four cysteine residues, Cys^{159} is the most reactive with EMA, its labeling being complete within 2 min at 0 °C in association with inhibition of the transport, while Cys^{56} and Cys^{256} are moderately reactive with EMA, but that Cys^{128} is not labeled by EMA owing to its location in the interior of the membrane segment (Majima et al., 1993). Therefore, incubation of the carrier with EMA for a short period such as 30 s resulted in the specific labeling of Cys^{159}, whereas longer incubation, such as 10 min, resulted in the labelings of Cys^{56} and Cys^{256} besides Cys^{159}.

Loop M1 containing Cys^{56}, loop M2 containing Cys^{159}, and loop M3 containing Cys^{256} are rich in positive charges with fewer negative charges (Aquila et al., 1982a). Thus intra- and intermolecular salt bridges as well as hydrogen bonds of these loops should be important for the function of the carrier, as suggested by Klingenberg (1992) and by us (Majima et al., 1993). In this connection, it is noteworthy that the transport substrates ADP and ATP, and the transport inhibitors CATR, BKA, and EMA, are all bulky compounds carrying plural negative charges. In a preliminary study, we found that divalent anionic eosin-Y, a non-SH-reactive analog of EMA, inhibited ADP transport and the labeling of Cys^{159} by EMA. From these results, we conclude that EMA first interacts electrostatically with a positive charge(s) of the loops and then labels cysteine residues. Of these loops, loop M2 is the primary site for noncovalent interaction with EMA (Majima et al.,1993).

In this study we found that the transport substrates ADP and ATP, and the transport inhibitors BKA and Pal-CoA, dose-dependently inhibit the labeling of Cys^{159} by EMA from the matrix side (Figures 3–5). These effects should be due to their interaction with loop M2. BKA was the most potent inhibitor, followed by Pal-CoA. The inhibitory effects of ADP and ATP on EMA binding were much less than that of BKA, due to their comparable affinities to that of EMA for loop M2. By incubation of the submitochondrial particles with EMA for 10 min, we could observe the effects of test compounds such as ADP and BKA on the EMA labelings of Cys^{56} and Cys^{256} as well as Cys^{159}. During 10-min incubations, BKA at a concentration that completely inhibited ADP transport very strongly inhibited the labelings by EMA of

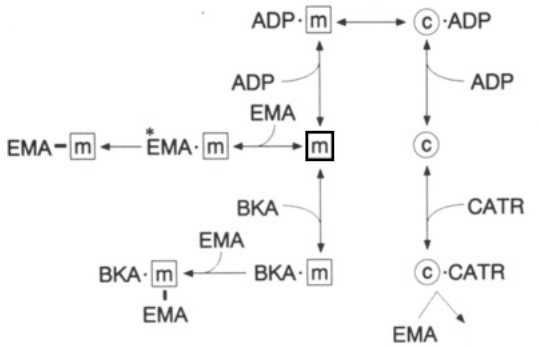

FIGURE 9: Schematic representation of interactions of the ADP/ATP carrier with ADP, CATR, BKA, and EMA. ADP (or ATP) binds with the ADP/ATP carrier in the c-state (c) on the cytosolic side and that in the m-state (m) on the matrix side (ADP·c and ADP·m, respectively). The reversible interconversion between these two states of the carrier is associated with nucleotide transport to the opposite side. CATR and BKA bind to the carrier in the c-state and m-state (CATR·c and BKA·m), respectively, and their bindings cause fixation of these states. Although EMA cannot bind to CATR·c, it labels Cys^{56} of BKA·m (BKA·m–EMA). EMA binds competitively with ADP to the m-state carrier from the matrix side (*EMA·m) and then labels the carrier (EMA–m) following the fixation of the carrier in the m-state. This model was constructed on the basis of the present results and the model proposed by Klingenberg (1989).

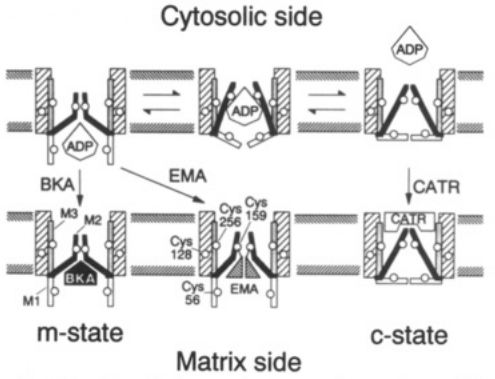

FIGURE 10: Postulated change in the conformations of loops M1, M2, and M3 of the ADP/ATP carrier in the dimer form under various conditions. Open circles represent cysteine residues. Open, solid, and stippled bars represent loops M1, M2, and M3, respectively. Hatched columns represent membrane segments. In this model, it is assumed that the dimer form of the carrier is responsible for transport activity, that six membrane segments in the monomer each consist of α-helices with about 20 amino acid residues, and that loops M1, M2, and M3 each consist of about 40 amino acid residues (Klingenberg, 1989; Majima et al., 1993), each with sufficient lengths to intrude deep into the membrane region, even though they form α-helices. However, they may not form α-helices, because the total α-helix content in the ADP/ATP carrier is reported to be only about 40%, being equivalent to the content in the 6 transmembrane helices in the six-transmembrane structure (Aquila et al., 1987).

Cys^{159} and Cys^{256}, but not the labeling of Cys^{56}. In contrast, ADP suppressed the labelings by EMA of Cys^{56} and Cys^{256}, and more significantly that of Cys^{159} (Figure 7).

The ADP/ATP carrier is known to take two different conformational states, the c-state and the m-state (Stubbs, 1981). As these two states are introduced by bindings of CATR and BKA, respectively, they are also referred to as the CATR state and BKA state (Brandolin et al., 1993). The transition of these two states is dependent on ADP or ATP: nucleotides on the cytosolic side bind to the carrier in the c-state conformation, and those on the matrix side to that in the m-state conformation, and then their transports to the opposite side induce the m-state and c-state, respectively, as shown in Figure 9. CATR on the cytosolic side and BKA on the matrix side lock the carrier in the c-state and the m-state, respectively (Klingenberg, 1989; Stubbs, 1981). From the finding that membrane-impermeable EMA did not label CATR-preloaded submitochondrial particles (Figure 2), EMA is thought not to bind to the carrier in the c-state. NEM, which has been shown to lock the transporter in the m-state conformation (Aquila et al., 1982b), mainly labels Cys^{56} (Majima et al., 1993), and treatment of mitochondria with NEM does not affect the binding of BKA (Aquila et al., 1982b). Furthermore, the predominant labeling of Cys^{159} by EMA is not affected by pretreatment with NEM (Majima et al., 1993), but was significantly suppressed by BKA, due to the higher affinity of BKA than EMA for loop M2 (Figure 7). From these results, it can be concluded that the noncovalent bindings of EMA and BKA to the carrier are essentially based on the same mechanism, and hence that the primary binding site of BKA is the loop M2, and the binding of EMA to loop M2, like that of BKA, locks the carrier in the m-state (Figure 9).

From the effects of ADP, CATR, and BKA on the labelings of the cysteine residues by EMA, we next considered the conformational changes of the three loops in relation to the transition between the c-state and m-state, as shown in Figure 10. Although other interpretations could be possible, this model, as our working hypothesis, well explains the present results as well as the results reported to date. In the previous report (Majima et al., 1993) we characterized three hydrophilic loops facing the matrix space from results on the labelings by EMA and NEM. We found that loop M1 is exposed to the matrix space, loop M2 is intruded into the membrane region, and loop M3 is intruded deep into the membrane (Majima et al., 1993). In our model (Figure 10), the conformational changes of the loops are based on the dimeric form of the carrier, with each monomer assumed to have a six-transmembrane structure (Klingenberg, 1989; Majima et al., 1993; Saraste & Walker, 1982). A dimeric form of the carrier as its functional unit is proposed from the results of binding of CATR (Riccio et al., 1975; Hachenberg & Klingenberg, 1980) and a neutron scattering study (Block et al., 1982), but the tetramer organization consisting of a pair of dimeric forms is also proposed to be a functional unit (Block & Vignais, 1984). The findings that azido-ADP (Dalbon et al., 1988), azido-ATP (Mayinger et al., 1989), and azido-ATR (Boulay et al., 1983), from the cytosolic side, and BKA from the matrix side, found in this study, all bind to loop M2 suggest that loop M2 is the primary binding site for ADP, ATP, ATR or CATR, and BKA. We consider that an intermolecular pair of membrane-intruded loops of M2 in the dimeric carriers functions as a primary gate, while the intermolecular pair of exposed loops M1 acts as an auxiliary secondary gate. Loop M3, which is thought to be intruded most deeply into the membrane, together with some transmembrane segments, could be essential members of the transport path. EMA on the matrix side will be predominantly attracted electrostatically to the positive charges in loop M2 (Majima et al., 1993), leading to its binding, opening the gate by cleavage of the salt bridge, and then labeling of Cys^{159}, which fixes the carrier in the m-state. Bound EMA would inhibit ADP transport by steric hindrance.

As shown in Figure 10, the binding of BKA to loop M2 causes closure of the primary gate formed by this loop, and hence EMA is not able to bind to Cys^{159}, and Cys^{256} deep in the membrane becomes inaccessible. In contrast, loop M1 containing Cys^{56} in the m-state exposed to the matrix space, and the binding of BKA to loop M2, does not cause any change in the exposed conformation of loop M1. Therefore, BKA does not have any effect on the labeling of Cys^{56} by EMA.

These conformations of the loops in the m-state caused by binding of BKA to loop M2 well explain why, in the m-state conformation, either Arg^{30} or Arg^{59} and Lys^{42} in loop M1 are susceptible to proteases (Brandolin et al., 1989; Marty et al., 1992), and Lys^{42} and Lys^{48} to pyridoxal 5-phosphate (Bogner et al., 1986). Membrane-impermeable CATR, which binds to the ADP/ATP carrier from the cytosolic side, almost completely inhibited the labeling by EMA of all the cysteine residues from the cytosolic side, and hence its binding could lock the carrier in the c-state, causing closure of the two gates. Therefore, the carrier fixed in the c-state conformation by CATR did not show any reactivity with NEM (Aquila & Klingenberg, 1982) and proteases (Brandolin et al., 1989; Marty et al., 1992). ADP in the matrix space, as in the present study, binds with positive charges of loop M2 in the m-state conformation competitively with EMA. These electrostatic interactions may cause a break in the salt bridge of the primary gate M2 and formation of a salt bridge of the secondary gate M1, leading to the transport of ADP to the cytosolic side (Figure 10). The reverse conformational change of the loops will take place when ADP or ATP is added to the cytosolic side leading, to its transport into the matrix space.

In conclusion, we propose that conformational changes of the loops of the ADP/ATP carrier regulate its transport activity. Further studies on the interactions between loops M2 and M1, and loops M2 and M3, are necessary for full understanding of the transport mechanism of ADP and ATP via the ADP/ATP carrier. We think that two loops and the N-terminal chain located on the cytosolic side are also important for the activity of the ADP/ATP carrier. Possibly, they act as gates on the cytosolic side like loop M1 on the matrix side.

ACKNOWLEDGMENT

We thank Dr. M. Klingenberg, University of Munich, for helpful discussion. We also thank Dr. J. A. Duine, Delft University of Technology, for a generous gift of bongkrekic acid and helpful suggestions.

REFERENCES

Aquila, H., & Klingenberg, M. (1982) *Eur. J. Biochem. 122*, 141–145

Aquila, H., Misra, D., Eulitz, M., & Klingenberg, M. (1982a) *Hoppe-Seyler's Z. Physiol. Chem. 363*, 345–349.

Aquila, H., Eiermann, W., & Klingenberg, M. (1982b) *Eur. J. Biochem. 122*, 133–139.

Aquila, H., Link, T. A., & Klingenberg, M. (1987) *FEBS Lett. 212*, 1–9.

Block, M. R., & Vignais, P. V. (1984) *Biochim. Biophys. Acta 767*, 369–376.

Block, M. R., Zaccaí, G., Lauquin, G. J. M., & Vignais, P. V. (1982) *Biochem. Biophys. Res. Commun. 109*, 471–477.

Bogner, W., Aquila, H., & Klingenberg, M. (1986) *Eur. J. Biochem. 161*, 611–620.

Boulay, F., Lauquin, G. J. M., Tsugita, A., & Vignais, P. V. (1983) *Biochemistry 22*, 477–484.

Brandolin, G., Boulay, F., Dalbon, P., & Vignais, P. V. (1989) *Biochemistry 28*, 1093–1100.

Brandolin, G., Le Saux, A., Trezeguet, V., Lauquin, G. J. M., & Vignais, P. V. (1993) *J. Bioenerg. Biomembr. 25*, 459–472.

Dalbon, P., Brandolin, G., Boulay, F., Hoppe, J., & Vignais, P. V. (1988) *Biochemistry 27*, 5141–5149.

Hackenberg, H., & Klingenberg, M. (1980) *Biochemistry 19*, 548–555.

Hansen, M., & Smith, A. L. (1964) *Biochim. Biophys. Acta 81*, 214–222.

Houstek, J., & Pedersen, P. L. (1985) *J. Biol. Chem. 260*, 6288–6295.

Klingenberg, M. (1980) *J. Membr. Biol. 56*, 97–105.

Klingenberg, M. (1989) *Arch. Biochem. Biophys. 270*, 1–14.

Klingenberg, M. (1992) *Biochem. Soc. Trans. 20*, 547–550.

Klingenberg, M. (1993) *J. Bioenerg. Biomembr. 25*, 447–457.

Laemmli, U. K. (1970) *Nature 227*, 680–685.

Lauquin, G. J. M., Villiers, C., Michejda, J. W., Hryniewiecka, L. V., & Vignais, P. V. (1977) *Biochim. Biophys. Acta 460*, 331–345.

Majima, E., Koike, H., Hong, Y.-M., Shinohara, Y., & Terada, H. (1993) *J. Biol. Chem. 268*, 22181–22187.

Marty, I., Brandolin, G., Gagnon, J., Brasseur, R., & Vignais, P. V. (1992) *Biochemistry 31*, 4058–4065.

Mayinger, P., Winkler, E., & Klingenberg, M. (1989) *FEBS Lett. 244*, 421–426.

Nelson, D. R., Lawson, J. E., Klingenberg, M., & Douglas, M. G. (1993) *J. Mol. Biol. 230*, 1159–1170.

Riccio, P., Aquila, H., & Klingenberg, M. (1975) *FEBS Lett. 56*, 133–138.

Saraste, M., & Walker, J. E. (1982) *FEBS Lett. 144*, 250–254.

Smith, A. L. (1967) *Methods Enzymol. 10*, 81–86.

Smyth, D. (1964) *Biochem. J. 91*, 589–595.

Stubbs, M. (1981) in *Inhibitors of Mitochondrial Functions* (Erecinska, M., & Wilson, D. F., Eds.) pp 283–304, Pergamon Press, Oxford.